

Comparative Study of the Structural, Mechanical, Electronic, Optical and Thermodynamic Properties of Superconducting Disilicide YT_2Si_2 (X=Co, Ni, Ru, Rh, Pd, Ir) by DFT Simulation

Md. Atikur Rahman^{a*}, Mahbub Hasan^a, Rukaia Khatun^a, Jannatul Ferdous Lubna^a, Sushmita Sarker^a, Md. Zahid Hasan, Wakil Hasan

DFT simulation based ab-initio approach has been executed for investigating the comparative study of the physical properties of superconducting disilicide materials YT_2Si_2 (T= Co, Ni, Ru, Rh, Pd, Ir). This is the first comparative theoretical investigation of these materials, which is done through Cambridge Serial Total Energy Package module. Extremely good relation has been observed between the synthesized and calculated structural parameters of all the superconductors. Mechanical structural stability of all the phases has been confirmed from the investigated elastic stiffness parameters. The investigated elastic moduli show good agreement with previously calculated data where available. Also the fundamental polycrystalline features such as bulk modulus, shear modulus, Young's modulus, Pugh's and Poison's ratios, ductile/brittle nature and hardness of superconducting YT_2Si_2 (T= Co, Ni, Ru, Rh, Pd, Ir) have been examined. Ductile nature of YRh_2Si_2 , YPd_2Si_2 and brittle nature of YCo_2Si_2 , YNi_2Si_2 , and YIr_2Si_2 have been observed from analyzing of polycrystalline elastic parameters where YRu_2Si_2 lies on the border line of ductile/brittle nature. The high bulk modulus, Young's modulus, and hardness of YIr_2Si_2 ensured that this phase has high ability to resist volume and plastic deformation and suitable in industrial applications. On the other hand the material the small Young's modulus of YPd_2Si_2 ensured its application as a thermal barrier coating (TBC) material. Metallic nature of YT_2Si_2 (T= Co, Ni, Ru, Rh, Pd, Ir) has been confirmed from the band structure and DOS calculations. Mulliken atomic populations and charge density map reveal the existing of covalent and ionic bond in YT_2Si_2 (T= Co, Ni, Ru, Rh, Pd, Ir). Different optical features included dielectric function, refractive index, optical conductivity, reflectivity, absorption and loss function of YT_2Si_2 (T= Co, Ni, Ru, Rh, Pd, Ir) have been executed through CASTEP code directly. The high reflectivity in the UV energy region of these phases ensured their application as good solar reflector in this energy site. Furthermore the thermodynamic properties of superconducting YT_2Si_2 (T= Co, Ni, Ru, Rh, Pd, Ir) have been determined from the elastic stiffness constants. The high conductivity of YCo_2Si_2 is ensured from its high Debye and melting temperature. The minimum thermal conductivity of YPd_2Si_2 ensured that it is suitable to use as a thermal barrier coating (TBC) material.

Keywords: DFT simulation; Superconducting Phases YT_2Si_2 (T= Co, Ni, Ru, Rh, Pd, Ir); Structural and Mechanical Properties; Electronic and Bonding Properties; Optical and Thermal Properties

Corresponding author: atik0707phy@gmail.com

1. Introduction

Superconducting materials are always demandable for their valuable applications in modern technology and the discovery of high T_c superconductors of several types of compounds has concerned huge attention in the recent time. The layered ternary compounds of 122 types belong to most inspiring and have been significantly studied by several researchers in several times. The 122 type ternary compounds have two types of structures; where one belong to body-centered tetragonal configuration ThCr_2Si_2 (space group $I4/mmm$) and the second one goes to primitive tetragonal structure CaBe_2Ge_2 (space group $P4/nmm$) [1]. There are more than seven hundred compounds fall in the ThCr_2Si_2 -type configuration with space group of $I4/mmm$ (139) [2-4]. At ambient condition the structure ThCr_2Si_2 is thermodynamically stable; on the other hand the structure CaBe_2Ge_2 is thermodynamically stable at high temperature. The general formula of ThCr_2Si_2 -type configuration is AT_2X_2 where A stand for alkali, alkaline earth or rare earth elements; T stand for 3d, 4d and 5d transition metals and finally X belongs to p-elements such as Si, Ge, As or P. The crystal structure of ThCr_2Si_2 -type was first synthesized and described by Ban and Sikirica in 1965 [5] however the theoretical simulation of ThCr_2Si_2 was first done by Shein and Ivanovskii in 2011 [6]. In 1996 Just and Pauer had give an entire geometric investigation of about 600 compounds of ThCr_2Si_2 -type configuration [4]. From past to present most researchers have been working on ThCr_2Si_2 -type compounds frequently for the reason that these types of compounds have several diversity of remarkable physical observable fact such as massive fermion character, superconductive manner (in high and low temperature), interesting magnetic order, assorted valency and valence instability, phase transition, Kondo effect etc [7-11]. The discovery of iron-based high T_c (up to 49 K) superconducting materials AFe_2As_2 ($A = \text{Ca, Ba, Sr, Eu}$) fall in the ThCr_2Si_2 -type configurations play a great role in the modern technology [12-14]. But it is so difficult to synthesis iron-based high T_c superconductors in practically. To overcome this situation researcher was looking to discover the alternative of iron- pnictides and have succeeded by finding the mixture of ternary intermetallic ThCr_2Si_2 -type compounds. The ideal ThCr_2Si_2 -type crystal structure is obtained from several layers created by edge-sharing network of BX_4 tetrahedral alternating with Ba ions [4]. Several iron-free compounds included CaPd_2Ge_2 ($T_c = 1.98$ K) [15], CaPd_2As_2 ($T_c = 1.27$ K) [16], SrPd_2Ge_2 ($T_c = 3.04$ K) [17], SrIr_2Ge_2 , SrNi_2Ge_2 ($T_c < 1.8$ K) [18], YIr_2Si_2 ($T_c = 2.52$ K) [19], BaNi_2P_2 ($T_c = 2.80$ K), BaIr_2P_2 ($T_c = 1.97$ K), BaRh_2P_2 ($T_c = 0.70$ K) [20], YPt_2Si_2 [21], YPd_2Si_2 and YRh_2Si_2 [22] show superconductive features with very low T_c (below 3K). Very recent Pt, Ni, and Pd-based ThCr_2Si_2 type boro-carbides [23-25] show superconductive phenomena with transition temperature up to 23K. In this research article we are focused to comparative investigation of the details physical features included mechanical, hardness, anisotropic manner, properties related to photon and temperature of superconducting disilicide YT_2Si_2 ($X = \text{Co, Ni, Ru, Rh, Pd, Ir}$) along with some similar types of compounds for the initial moment. The studied compounds YT_2Si_2 ($T = \text{Co, Ni, Ru, Rh, Pd, Ir}$) belong to ternary layered ThCr_2Si_2 -type tetragonal configurations where the set of lattice points fall in the space group $I4/mmm$ (139) [21]. The compound YCo_2Si_2 was initially examined by Rossi *et al.* in 1978 via the X-ray powder diffraction method [26].

Höting et al. synthesized the silicides YT_2Si_2 ($T = Co, Ni, Cu, Ru, Rh, Pd$) by Solid-state NMR Spectroscopy in 2014 [27] where all the compounds go to $ThCr_2Si_2$ -type structure. After reviewing the literature we have observed that only the theoretical study is performed on YIr_2Si_2 by I.R. Shein in 2011 [28] among all the studied compounds. No theoretical works on YT_2Si_2 ($T = Co, Ni, Ru, Rh, Pd$) are available in the literature yet. However a lot of theoretical works on the $ThCr_2Si_2$ -type compounds are performed by several researchers in several times. M. U. Salma *et al.* studied the physical features of ARh_2Ge_2 ($A = Ca, Sr, Y$ and Ba) in 2019 [29] through DFT simulation. In 2019 Chowdhury *et al.* investigated the details physical features of $ThCr_2Si_2$ -type Ru-based materials $SrRu_2X_2$ ($X = P, Ge, As$) through ab-initio method [30]. Rahaman *et al.* studied the physical properties of Ir-based superconductors $BaIr_2Mi_2$ ($Mi = P$ and As) [31] and Ru-based superconductors $LaRu_2M_2$ ($M = P$ and As) [32] in 2017 using *ab-initio* method. In our previous study we have investigated the physical properties of Ni-based superconductors $BaNi_2T_2$ ($T = P, As$) [33] and $SrNi_2M_2$ ($M = As$ and Ge) [34] in 2019. In 2019 Ali *et al.* discover the physical features of Pd-based superconductors XPd_2Ge_2 ($X = Ca, Sr, La, Nd$) [35]. Though remarkable efforts have been done to synthesis and discover the superconducting features of disilicides YT_2Si_2 ($T = Co, Ni, Ru, Rh, Pd, Ir$), there is still missing of detail theoretical works included electronic, mechanical, thermal and optical properties these superconductors in literature. On the basis of having important crystal features and practical applications of compounds YT_2Si_2 ($T = Co, Ni, Ru, Rh, Pd, Ir$) we therefore decided to study the all the physical attributes of these compounds employing the DFT simulation based on CASTEP code. Not only that we have tried to compare the investigated results with some similar type of compounds which are already available in literature. We think that this study will play an important role in the research area and superconductor based modern technology.

2. Computational Details

Employing Density Functional Theory (DFT) [36] we have examined the structural features, stability factors named elastic stiffness parameters, hardness, band structures, light and temperature related properties of superconducting disilicides YT_2Si_2 ($T = Co, Ni, Ru, Rh, Pd, Ir$) for first time. All the features are executed by CASTEP code [37]. The generalized gradient approximation (GGA) was used to estimate the exchange correlation functional energy accompanied with the Perdew-Burke-Ernzerhof functional (PBE) [38]. The Vanderbilt-type ultrasoft pseudopotential [39] was employed to describe the interactions happened between electrons and ions. We have sampled the Brillouin-zone using Monkhorst-Pack grids [40] of $14 \times 14 \times 6$ with a plane wave cut-off energy of 500 eV for YCo_2Si_2 and YIr_2Si_2 and $16 \times 16 \times 7$ with a plane wave cut-off energy of 520 eV for YT_2Si_2 ($T = Ni, Ru, Rh, Pd$) respectively. For searching the ground state of all the phases geometry optimization has been performed utilizing BFGS (Broyden-Fletcher-Goldfarb-Shanno) relaxing technique [41]. For the geometry optimization the convergence tolerance was fixed to ultra-fine quality along with energy of 5.0×10^{-6} eV/atom, maximum force of $0.01 \text{ eV}/\text{\AA}$, maximum stress of 0.02 GPa and maximum displacement of 5.0×10^{-4} Å. At the optimized structures the elastic stiffness constants are investigated using the finite

stress-strain method [42] according to Hock's law. The 2D and 3D anisotropy contours are investigated through the ELATE code [43]. Photon related optical features of superconducting YT_2Si_2 ($T=Co, Ni, Ru, Rh, Pd, Ir$) have been studied by employing the CASTEP code [42] directly. The temperature dependent thermodynamic properties are calculated by utilizing the elastic stiffness constants.

3. Results and discussion

3.1 Structural Properties

The superconducting yttrium silicides YT_2Si_2 ($T= Co, Ni, Ru, Rh, Pd, Ir$) belong to ternary layered $ThCr_2Si_2$ -type tetragonal configurations through space group of $I4/mmm$ (139) [27]. Utilizing the synthesized lattice parameters we have drawn the conventional crystal structure of YT_2Si_2 ($T= Co, Ni, Ru, Rh, Pd, Ir$) which is displayed in Fig. 1 (a). Fig. 1(b) show the crystal structure of YT_2Si_2 ($T= Co, Ni, Ru, Rh, Pd, Ir$) which is attained after the geometry optimization. The unit cell of all the crystal structures contains two formula units with 10 atoms. In the unit cell of YT_2Si_2 ($T= Co, Ni, Ru, Rh, Pd, Ir$) the Y atom takes the position 2a (0 0 0), Co/Ni/Ru/Rh/Pd/Ir atoms are in the sites 4d (0 0.5 0.25) and at last the Si atom located at the sites 4e (0 0 z_{Si}) where z represents the internal parameter. The primitive cell has one formula unit containing 5 atoms. The synthesized unit cell dimensions, atomic positions, Wyckoff positions, lattice parameters after optimization and cell volumes are listed in Table 1. The values of the investigated structural parameters are very close to the synthesized data confirming the accuracy of the present simulations.

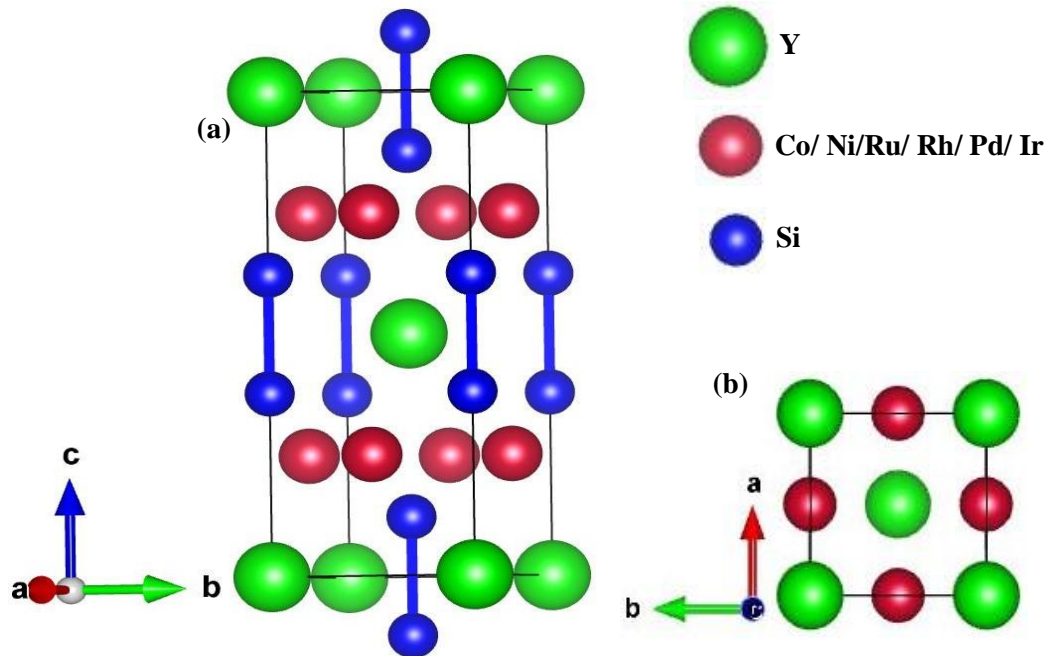


Fig.5.1. (a) Conventional 3D, and (b) the optimized 2D crystal structures of YT_2Si_2 ($T= Co, Ni, Ru, Rh, Pd, Ir$).

Table 1: Optimized lattice constants a , c (in Å) and cell volume V (in Å³) of superconducting YT₂Si₂ (T= Co, Ni, Ru, Rh, Pd, Ir) polymorphs.

Compounds	$a = b$ (Å)	c (Å)	$V = a^2c$ (Å ³)	Atomic positions [27]					Ref.
				Wyckoff	Element	x	y	z	
YCo ₂ Si ₂	3.889	9.864	149.1863	2a	Y	0	0	0	This study
				4d	Co	0	0.5	0.25	
				4e	Si	0	0	0.373	
	3.8875	9.734	147.1066						[27]
YNi ₂ Si ₂	3.980	9.638	152.6698	2a	Y	0	0	0	This study
				4d	Co	0	0.5	0.25	
				4e	Si	0	0	0.374	
	3.955	9.568	149.6629						[27]
YRu ₂ Si ₂	4.177	9.708	169.3787	2a	Y	0	0	0	This study
				4d	Co	0	0.5	0.25	
				4e	Si	0	0	0.368	
	4.158	9.546	165.0405						[27]
YRh ₂ Si ₂	4.085	10.068	168.007	2a	Y	0	0	0	This study
				4d	Co	0	0.5	0.25	
				4e	Si	0	0	0.378	
	4.018	9.897	159.7804						[27]
YPd ₂ Si ₂	4.152	9.992	172.2531	2a	Y	0	0	0	This study
				4d	Co	0	0.5	0.25	
				4e	Si	0	0	0.383	
	4.128	9.857	167.9671						[27]
YIr ₂ Si ₂	4.081	10.046	167.3117	2a	Y	0	0	0	This study
				4d	Co	0	0.5	0.25	
				4e	Si	0	0	0.364	
	4.048	9.815	160.8316						[27]

3.2 Stiffness constants and mechanical insights

The elastic constants give a compressive understanding of how solid materials behave mechanically and dynamically. Several elementary solid-state phenomena such as nature of bonding existence between atoms, EOS and Phonon spectra are directly related to the elastic features [44]. These constants elaborate about a solid's stability, brittleness, anisotropy, ductility, and stiffness nature of materials [45]. Due to crystal symmetry a tetragonal crystal system contain six independent elastic constants namely; C_{11} , C_{12} , C_{13} , C_{33} , C_{44} and C_{66} . The investigated results of the studied materials along with similar types of compounds are provided in Table 2. Elastic constants must meet Born criterion for tetragonal crystal structure [46].

$$\left. \begin{aligned} C_{11} > 0, C_{44} > 0, C_{33} > 0, C_{66} > 0 \\ C_{11} + C_{33} - 2C_{13} > 0, C_{11} - C_{12} > 0 \\ 2(C_{11} + C_{12}) + C_{33} + 4C_{13} > 0 \end{aligned} \right\} \quad (1)$$

It is clear from **Table 2** that all the six materials YCo₂Si₂, YNi₂Si₂, YRu₂Si₂, YRh₂Si₂, YPd₂Si₂ and YIr₂Si₂ are mechanically stable in view of the fact that they fulfilled the above criteria.

Table 2: Calculated elastic constants (C_{ij} , in GPa) of superconducting YT_2Si_2 (T=Co, Ni, Ru, Rh, Pd, Ir) polymorphs along with similar types of compounds.

Compounds	C_{11}	C_{12}	C_{13}	C_{33}	C_{44}	C_{66}	Ref.
YCo ₂ Si ₂	265.59	85.51	97.45	238.82	113.55	117.97	This study
YNi ₂ Si ₂	239.88	54.81	94.01	248.98	97.36	56.81	
YRu ₂ Si ₂	266.88	97.56	93.87	222.26	78.87	114.27	
YRh ₂ Si ₂	256.03	124.66	105.12	257.14	95.59	122.91	
YPd ₂ Si ₂	215.70	67.01	118.47	234.04	75.98	47.79	
YIr ₂ Si ₂	333.20	140.95	102.28	302.25	112.00	153.64	
	313.00	130.00	98.00	305.00	99.00	14.00	[19]
BaNi ₂ P ₂	171.91	21.23	66.51	89.25	43.84	23.04	[33]
BaIr ₂ P ₂	241.36	106.68	47.12	119.82	30.05	124.97	[31]
BaRh ₂ Ge ₂	145.7	61.1	39.6	46.5	36.80	66.1	[29]
SrRu ₂ P ₂	222.22	90.34	47.30	78.38	35.40	121.26	[30]
LaRu ₂ P ₂	277.52	104.54	72.26	116.39	50.64	132.75	[32]
LaPd ₂ Ge ₂	178.36	49.78	89.53	157.90	54.46	32.29	[35]
YRh ₂ Ge ₂	217.0	86.9	98.4	201.0	47.5	74.9	[29]

Other basic parameters, called polycrystalline bulk moduli, like bulk modulus B , Shear modulus G , Young's modulus E , Pugh's ratio B/G , B/C_{44} , and H_v , are very important for describing the mechanical features of materials, such as material's strength, ductility/brittleness, stiffness, ability to be machined, hardness, and so on. Table 3 contains of all of the bulk parameters, along with the value found in the previous investigation of similar 122 type's superconducting materials for comparative study [29-33]. Using the calculated elastic constants, the bulk modulus, shear modulus, Young's modulus, anisotropy, and hardness of superconducting YT_2Si_2 (T=Co, Ni, Ru, Rh, Pd, Ir) are determined by the Voigt-Reuss-Hill approximations [47]. Based on the Voigt-Reuss-Hill approximations, the bulk and shear modulus for tetragonal crystal system are as follows:

$$B_V = \frac{2C_{11} + 2C_{12} + C_{33} + 4C_{13}}{9} \quad (2)$$

$$B_R = \frac{C^2}{M} \quad (3)$$

$$G_V = \frac{M + 3C_{11} - 3C_{12} + 12C_{44} + 6C_{66}}{30} \quad (4)$$

$$G_R = \frac{15}{\left[\frac{18B_V}{C^2} + \frac{6}{(C_{11}-C_{12})} + \frac{6}{C_{44}} + \frac{3}{C_{66}} \right]} \quad (5)$$

Where, $M = C_{11} + C_{12} + 2C_{33} - 4C_{13}$ and $C^2 = (C_{11} + C_{12})C_{33} - 2C_{13}^2$.

The average value of B and G given taken by Hill is giving by the following two relations,

$$B = \frac{1}{2}(B_R + B_v) \quad (6)$$

$$G = \frac{1}{2}(G_v + G_R) \quad (7)$$

Now we can calculate the Young's modulus (E), and Poisson's ratio (ν) from the relations below,

$$E = \frac{9GB}{3B + G} \quad (8)$$

$$\nu = \frac{3B - 2G}{2(3B + G)} \quad (9)$$

The anisotropic behaviors of a crystal can be estimated by the following equation [48],

$$A^U = \frac{5G_V}{G_R} + \frac{B_V}{B_R} - 6 \quad (10)$$

The hardness of materials can be predicted by using the following relation [49],

$$H_V = 2(K^2 G)^{0.585} - 3 \quad (11)$$

Table 3: Calculated polycrystalline elastic constants (C_{ij} , in GPa) and hardness, H_V (GPa) of superconducting YT_2Si_2 ($T=Co, Ni, Ru, Rh, Pd, Ir$) polymorphs along with similar types of compounds.

Phases	B_V	B_R	B	G_V	G_R	G	E	H_V	Ref.
YCo_2Si_2	147.87	147.76	147.81	101.65	98.28	99.97	244.74	15.72	This study
YNi_2Si_2	134.93	133.69	134.31	82.70	78.76	80.78	201.88	11.40	
YRu_2Si_2	147.41	146.21	146.81	85.78	83.50	84.64	212.99	11.09	
YRh_2Si_2	159.88	159.72	159.81	91.77	87.13	89.79	226.88	11.15	
YPd_2Si_2	141.48	137.57	139.53	64.05	60.26	62.16	162.37	5.70	
YIr_2Si_2	184.41	182.80	183.61	117.07	114.13	115.60	286.64	15.74	[19]
	175.90	175.40	175.60	82.70	45.30	64.00	171.20	3.99	
$BaNi_2P_2$	-	-	80.92	-	-	35.87	93.77	3.27	[33]
$BaIr_2P_2$	-	-	102.46	-	-	55.04	140.04	6.92	[31]
$BaRh_2Ge_2$	68.72	45.83	57.30	41.11	31.89	36.50	90.3	3.56	[29]
$SrRu_2P_2$	99.19	71.48	85.33	60.94	45.87	53.40	132.55	8.83	[30]
$LaRu_2P_2$	-	-	117.19	-	-	68.15	171.25	9.53	[32]
$LaPd_2Ge_2$	-	-	107.80	-	-	45.26	119.11	3.74	[35]
YRh_2Ge_2	133.60	133.59	133.60	57.40	55.53	56.50	148.6	7.09	[29]

The fundamental bulk characteristic B , defined as volume stress to volume strain, reveals a material's ability to resist plastic deformation. A high value for B indicates that the material is capable of resisting significant amounts of plastic or volume deformation. From Table 3 and Fig. 2(b) we have observed that among that all the compounds, YIr_2Si_2 has a highest value of B , which ensured that this phase is more capable to resist plastic deformation. The sequence of bulk modulus of all the compounds listed in Table 3 is $YIr_2Si_2 > YRh_2Si_2 > YCo_2Si_2 > YRu_2Si_2 > YNi_2Si_2 > YPd_2Si_2 > YRh_2Ge_2 > LaRu_2P_2 > LaPd_2Ge_2 > BaIr_2P_2 > SrRu_2P_2 > BaNi_2P_2 > BaRh_2Ge_2$. From this analysis we have seen that the studied compounds YT_2Si_2 ($T=Co, Ni, Ru, Rh, Pd, Ir$) have more ability to resist plastic deformation than the previous studied materials [29-35].

The shear modulus, G , is another essential bulk factor that determines the material's resistance to shear deformation as the ratio of shear stress to shear strain. From Table 3 and Fig. 2(b), we can see that YIr_2Si_2 has a higher G than the other compounds listed in Table 3, which means it can resist shear deformation better than the others. The sequence of shear modulus of the studied compounds is $\text{YIr}_2\text{Si}_2 > \text{YCo}_2\text{Si}_2 > \text{YRh}_2\text{Si}_2 > \text{YRu}_2\text{Si}_2 > \text{YNi}_2\text{Si}_2 > \text{YPd}_2\text{Si}_2$.

Young's modulus, E , is a crucial bulk quantity that assesses a material's resistance to longitudinal stress. In addition, it has managed the thermal shock resistance of a periodic crystal. The system where E is inversely proportional to R is referred to as the crucial thermal shock coefficient [50], which indicates that the lower the value of E , the greater the resistance to thermal shock. Here the lower value of YPd_2Si_2 ensured that it has high ability to resist the thermal shock than the other compounds studied (Table 3 and Fig. 2(b)) in this work. Comparing among all the compounds as shown in Fig. 2(b) and Table 3, we can see that the phase YIr_2Si_2 has highest E value indicating that this phase has highest ability to resist longitudinal stress than all the rest ones. On the other hand, BaRh_2Ge_2 has the smallest value of E among all of the phases (see Fig. 2(b)), which indicates that BaRh_2Ge_2 is more suitable to be employed as a thermal barrier coating (TBC) material compared to others. The Young's modulus sequence of all the compounds is $\text{YIr}_2\text{Si}_2 > \text{YCo}_2\text{Si}_2 > \text{YRh}_2\text{Si}_2 > \text{YRu}_2\text{Si}_2 > \text{YNi}_2\text{Si}_2 > \text{YPd}_2\text{Si}_2 > \text{LaRu}_2\text{P}_2 > \text{YRh}_2\text{Ge}_2 > \text{BaIr}_2\text{P}_2 > \text{SrRu}_2\text{P}_2 > \text{LaPd}_2\text{Ge}_2 > \text{BaNi}_2\text{P}_2 > \text{BaRh}_2\text{Ge}_2$.

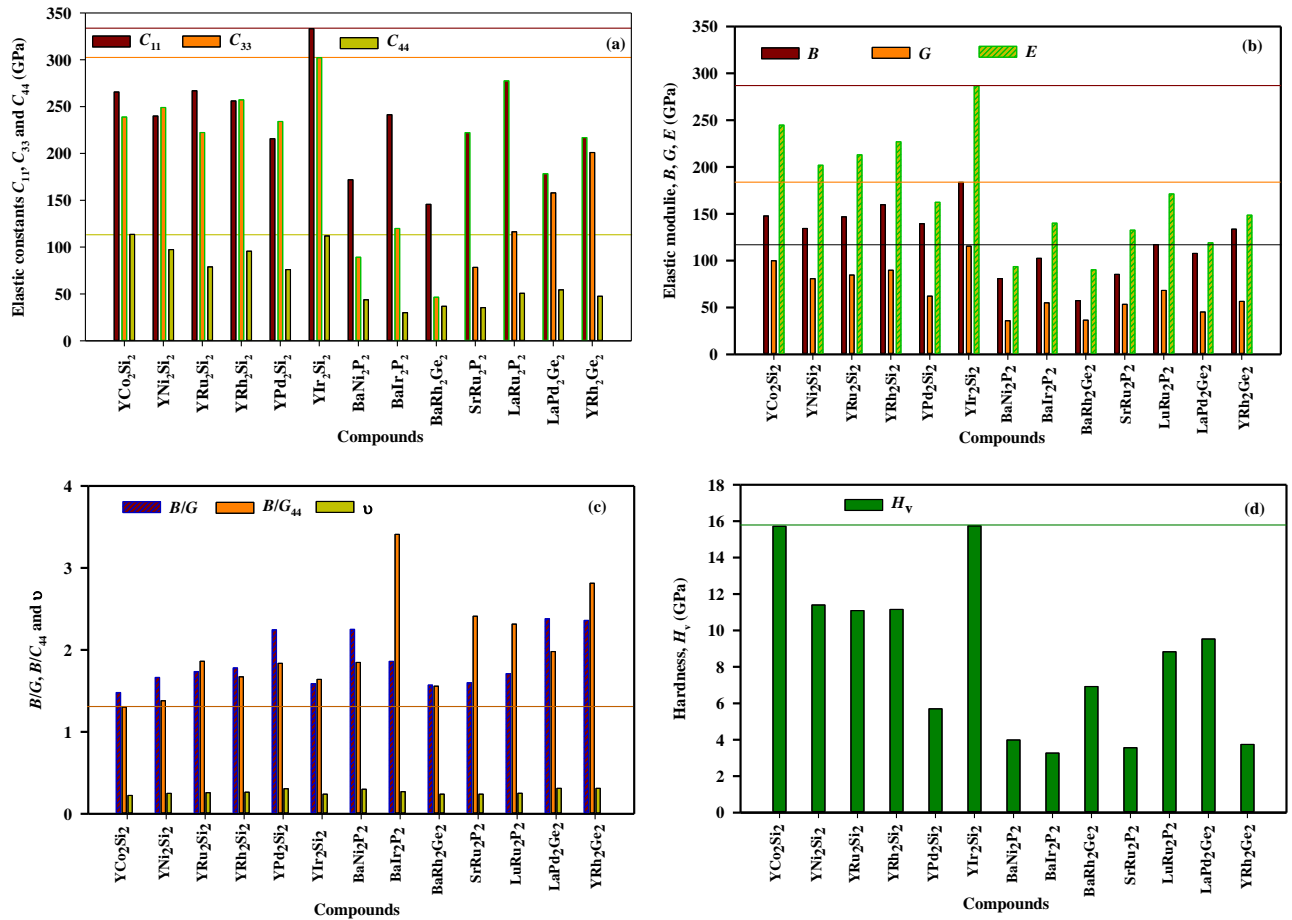


Fig. 2: Bulk features of superconducting YT_2Si_2 ($\text{T}=\text{Co}, \text{Ni}, \text{Ru}, \text{Rh}, \text{Pd}, \text{Ir}$).

Table 4: Calculated Pugh's ratio (B/G), Poisson's ratio (ν), machinability index ($\mu = B/C_{44}$), elastic anisotropic factors (A and A^U) of superconducting YT_2Si_2 ($T=Co, Ni, Ru, Rh, Pd, Ir$) polymorphs with some 122 type superconductors.

Phases	Status	B/G	ν	B/C_{44}	A	A^U	Ref.
YCo_2Si_2	Brittle	1.479	0.224	1.302	1.261	0.173	This study
YNi_2Si_2	Brittle	1.663	0.249	1.379	1.052	0.259	
YRu_2Si_2	Brittle	1.735	0.258	1.861	0.932	0.145	
YRh_2Si_2	Ductile	1.780	0.263	1.672	1.455	0.227	
YPd_2Si_2	Ductile	2.245	0.306	1.836	1.022	0.343	
YIr_2Si_2	Brittle	1.588	0.239	1.639	1.269	0.138	
$BaNi_2P_2$	Ductile	2.25	0.30	1.846	0.582	1.600	[33]
$BaIr_2P_2$	Ductile	1.86	0.27	3.409	0.446	2.090	[31]
$BaRh_2Ge_2$	Brittle	1.57	0.24	1.557	0.869	1.945	[29]
$SrRu_2P_2$	Brittle	1.60	0.24	2.410	0.537	2.020	[30]
$LaRu_2P_2$	Brittle	1.71	0.25	2.314	0.586	1.350	[32]
$LaPd_2Ge_2$	Ductile	2.38	0.31	1.979	0.847	0.480	[35]
YRh_2Ge_2	Ductile	2.36	0.31	2.813	0.730	0.168	[29]

In order to predict whether a material would be ductile or brittle, scientist Pugh used a formula between bulk modulus and shear modulus (B/G): if B/G is greater than 1.75, the material in question would be ductile, otherwise it would be brittle [8]. Another important bulk parameter known as Poisson ratio, ν predict the ductile/brittle nature of material. According to this rule a material will show ductile/brittle nature when the value of ν will be $\nu > 0.26$ and $\nu < 0.26$ respectively [9]. According to above criteria the studied compounds YCo_2Si_2 , YNi_2Si_2 , and YIr_2Si_2 show brittle nature and YRh_2Si_2 and YPd_2Si_2 show ductile nature (see **Table 3** and **Fig. 3**) where YRu_2Si_2 lies on the brittle/ductile border line.

The machinability of a material is a key consideration in today's industrial sector, where the goal is to maximize output while minimizing expenses. The machinability index is influenced by a wide variety of factors, including the cutting form, the type of cutting, the rigidity, the hardness, and the capacity of the machine tool [10]. This useful parameter is denoted by μ and defined [11] by the ratio of bulk modulus, B to shear resistance, C_{44} i.e

$$\mu = B/C_{44} \quad (13)$$

This index also measures the material's lubricating properties and its plasticity [12-13]. High B/C_{44} means that a material has great lubricating properties, little friction, and a high plastic strain. From **Fig. 2 (c)** it is very clear that among the six materials YRu_2Si_2 has high machinability index indicating that it is very good machinable than all the others materials. The findings of this study are intriguing because they show that materials with low bulk, Young's, and shear moduli still have very high machinability and can be effectively used in industry.

Elastic anisotropy factor, A , also known as the Zener anisotropy factor, defines the bulk properties of a crystal system that depend on direction. If the properties of a crystal are uniform in all directions, then the crystal is isotropic; if the attributes vary in different directions, the crystal is anisotropic. The factor $A=1$ indicates the isotropic nature of a crystal, in other cases the crystal will be anisotropic. From our calculations we can say that all the compounds show anisotropic nature according to above criteria, where YRh_2Si_2 exhibits the largest anisotropic nature among the studied compounds.

Material hardness is another macroscopic bulk parameter that has a lot of uses in business and technology. A material with a high hardness has a greater capacity to withstand plastic deformation than one with a low hardness which is appropriate for plastic deformation and it becomes more machinable. A material will be more machinable and damage-tolerant when the value of hardness lies between 2 to 8 [14]. Analyzing **Fig. 2(d)** we can say that the material YIr_2Si_2 has highest hardness compared to other five compounds under study indicating that it has highest ability to resist plastic deformation than rest compounds. Consequently the low hardness of YPd_2Si_2 among the six components and among the ten compounds BaIr_2P_2 confirming that it is more machinable as shown in **Fig. 2 (d)**.

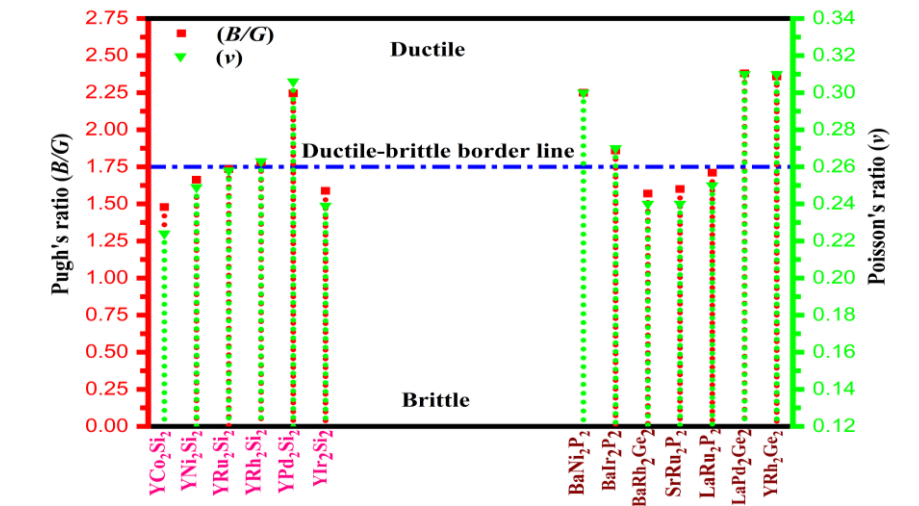


Fig. 3: Ductile/brittle nature of superconducting YT_2Si_2 ($T=\text{Co, Ni, Ru, Rh, Pd, Ir}$).

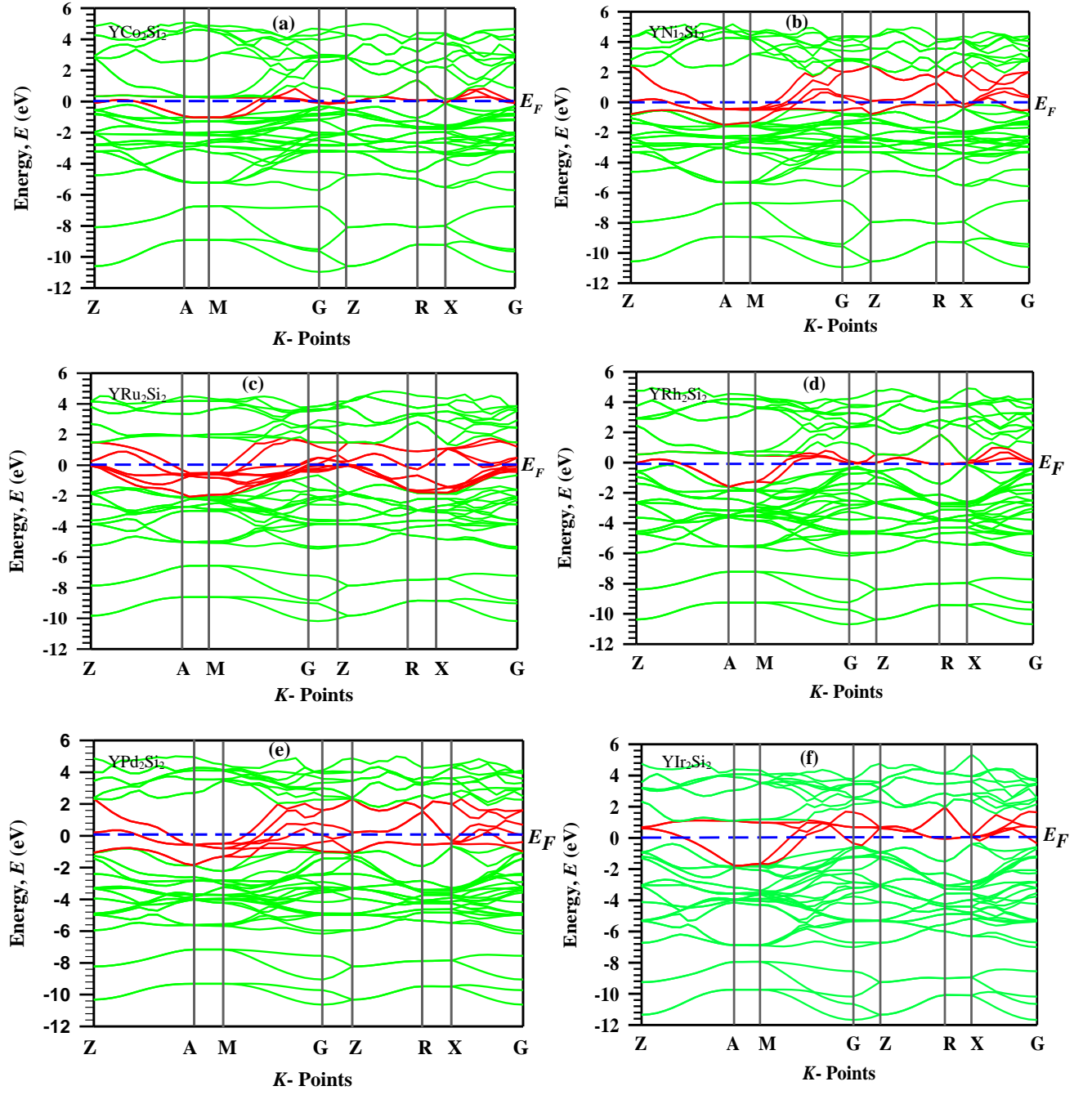


Fig. 4: Electronic Band structures of superconducting silicides YT_2Si_2 ($T=\text{Co, Ni, Ru, Rh, Pd, Ir}$).

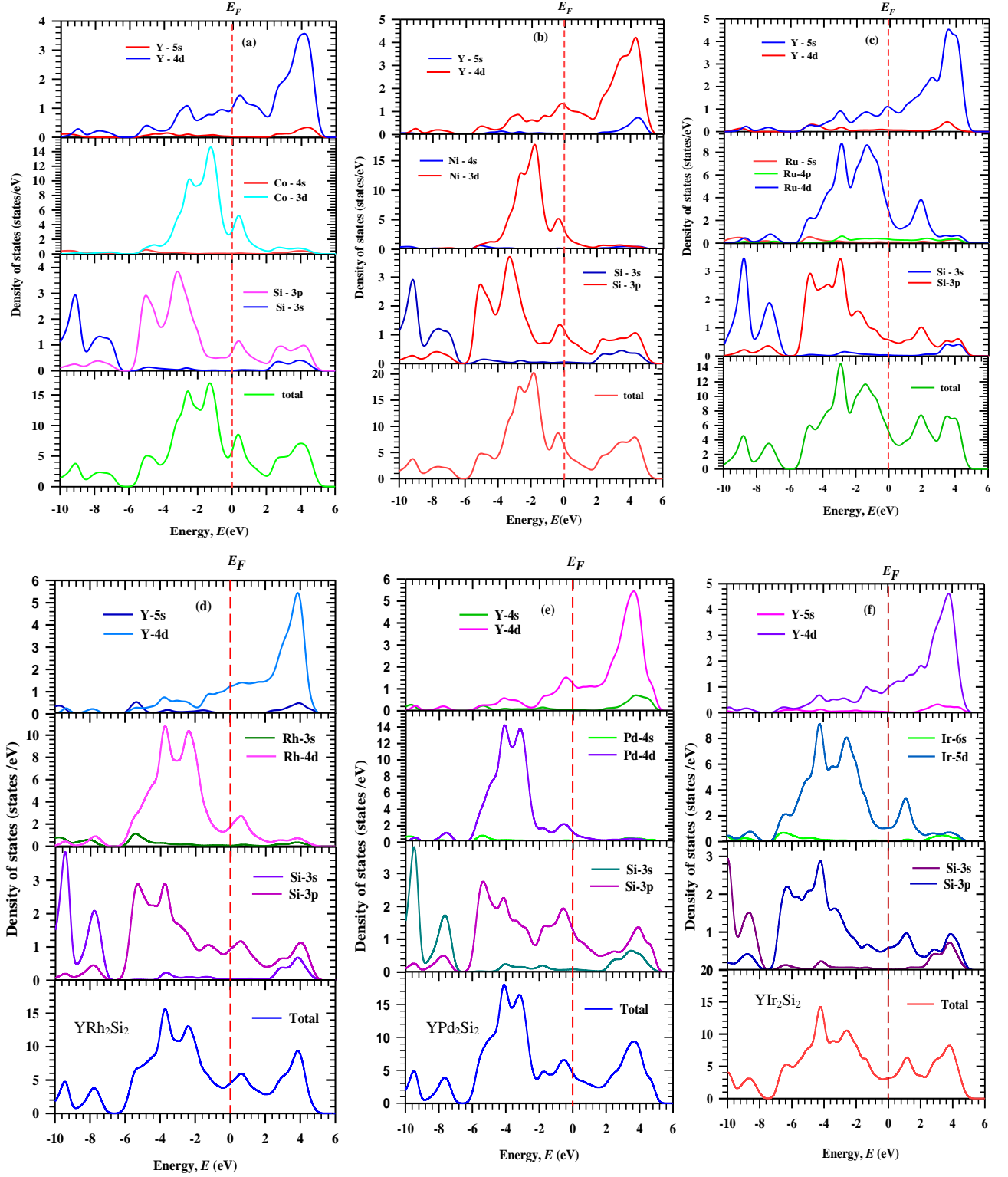


Fig. 5: Total and partial density of states of superconducting silicides YT_2Si_2 ($T=Co, Ni, Ru, Rh, Pd, Ir$).

5: Optical Properties

To gain insight into the electronic structure of the material the optical properties is one of the most important techniques. We have discussed the optical properties of YT_2Si_2 ($X=Co, Ni, Ru, Rh, Pd, Ir$) compounds in this section. To predict the optical function of YT_2Si_2 ($X=Co, Ni, Ru, Rh, Pd, Ir$) with various phonon energies [79] we have used the frequency-dependent dielectric function $\varepsilon(\omega) = \varepsilon_1(\omega) + i\varepsilon_2(\omega)$, which is closely related to the electronic configuration where the real $\varepsilon_1(\omega)$ and imaginary $\varepsilon_2(\omega)$ dielectric functions are correlated by the Kramers-Kronig relation. The real part $\varepsilon_1(\omega)$ can be calculated by the equation [80],

$$\varepsilon_1(\omega) = 1 + \frac{2}{\pi} P \int_0^{\infty} \frac{\omega' \varepsilon_2(\omega')}{\omega'^2 - \omega^2} d\omega' \quad (14)$$

Where ω is for the light frequency and P for the principle value of the integral part. The real $\varepsilon_1(\omega)$ and imaginary $\varepsilon_2(\omega)$ dielectric functions is obtained from the momentum matrix elements and taking into account every possible transition between the occupied and unoccupied electronic state, the imaginary part $\varepsilon_2(\omega)$ is calculated directly using [81]-

$$\varepsilon_2(\omega) = \frac{2e^2\pi}{\Omega\varepsilon_0} \sum_{k,v,c} |\psi_k^c| u \cdot r |\psi_k^v|^2 \delta(E_k^c - E_k^v - E) \quad (15)$$

Where ψ_k^c and ψ_k^v are the wave function at conduction and valence band, u denotes a vector defining the polarization of the incident electric field, e is denoted as the electric charge and ω denotes the light frequency respectively. The optical functions of YT_2Si_2 ($X=Co, Ni, Ru, Rh, Pd, Ir$) are estimated for phonon energies up to 20 eV which are shown in **Fig.11**. We have used 0.5 eV Gaussian smearing for all calculations because it spreads out of the Fermi level so that k-points are more efficient on the Fermi surface.

Fig.10(a) and **10(b)** show the expected real and imaginary parts of dielectric functions for all phases respectively. The large negative value of $\varepsilon_1(\omega)$ for any of these phases implies Drude-like metallic behavior. From above the imaginary portion $\varepsilon_2(\omega)$ approaches to zero, while the real part $\varepsilon_1(\omega)$ reaches through zero from below also show metallic nature. The plasma frequency 4 eV and damping (relaxation) energy 0.05 eV have been used. The main characteristics of our measured optical spectra of YT_2Si_2 ($X=Co, Ni, Ru, Rh, Pd, Ir$) are remarkably comparable, despite some variation in peak heights and locations.

The refractive index, which has no dimensions, quantifies and which is defined as how much light is bent or refracted as it enters a substance [88]. The idea of the refractive index of an optical material is significant for its use in optical tools such as photonic crystals, waveguides etc. **Fig. 10(c)** and **10(d)** display the refractive indices (real and imaginary portion) of the YT_2Si_2 ($X=Co, Ni, Ru, Rh, Pd, Ir$) compounds. The similar contribution found for all compounds in the whole graph. Both the phases

process the high refractive index in the infrared and visible area and ultraviolet regions these values are gradually decreased.

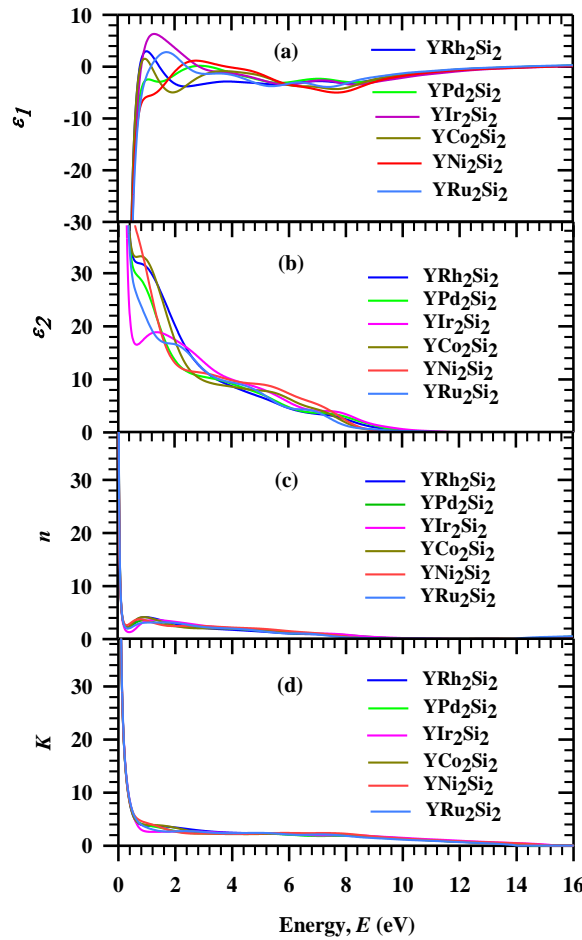


Fig. 10: (a and b) Dielectric functions, (c) refractive indices and (d) extension coefficient of YT_2Si_2 ($T=Co, Ni, Ru, Rh, Pd, Ir$).

The absorption coefficient is a necessary factor that indicates how much light of specific energy (wavelength) can enter a material before being absorbed, and it provides information on solar energy conversion efficiency. In **Fig.11(a)** absorption spectra for YT_2Si_2 ($X=Co, Ni, Ru, Rh, Pd, Ir$) are shown and they all start at 0 eV because their metallic nature,. According to **Fig. 11(a)**, for all of these compounds, the nature of the absorption curve is same, and many absorption peaks were found at various energy levels. However, all of these compounds possess good absorption coefficient.

Conductivity of a material refers to the ability to transport electron with the variation of photon energy [82]. It helps us to identify the material will be conductor, semiconductor or superconductor. The investigated conductivity spectra of YT_2Si_2 ($X=Co, Ni, Ru, Rh, Pd, Ir$) with photon energy are shown in **Fig.11(b)**. From this figure it has been seen that photoconductivity starts with zero photon energy due to the reason that the materials have no band gap which is evident from the band structure indicating the

metallic behaviors of these phases at energy 7.5eV the conductivity shows higher value; after that it gradually decreases and after energy about 13eV the conductivity vanishes for all compounds.

Reflectivity is the measure of light reflected by the materials upon incident on it. It is obtained by the ratio of the energy of the wave reflected from a surface to the energy of the wave incident on the surface [83]. The reflectivity of YT_2Si_2 ($X=Co, Ni, Ru, Rh, Pd, Ir$) as a function of photon energy is illustrated in Fig.11(c). It has been seen that reflectivity starts from 0.68 for YNi_2Si_2 and all other phases have the roughly similar spectra and the reflectivity starts between (5.2-6.2) eV with zero photon energy. The observed value represents good reflectivity in infrared and visible region. In ultraviolet region the absorption coefficient gradually decreases.

The energy loss function is a key factor in the dielectric formalism, which is utilized to clarify the optical dielectric formalism, which is utilized to clarify the optical created by fast charges in solid material. It is defined as the energy loss by a fast electron when it traverses in the material [84]. The frequency at which maximum energy loss happened is known as the bulk plasma frequency ω_p of the material which emerges at $\epsilon_2(\omega) < 1$ and $\epsilon_1(\omega) = 0$ [85–87]. The energy loss spectra show that all phases have the roughly similar plasma frequency ω_p with the approximated value (13-15.2)eV respectively indicating that all phases will be transparent when the incident photon energies are greater than (13-15.2) eV.

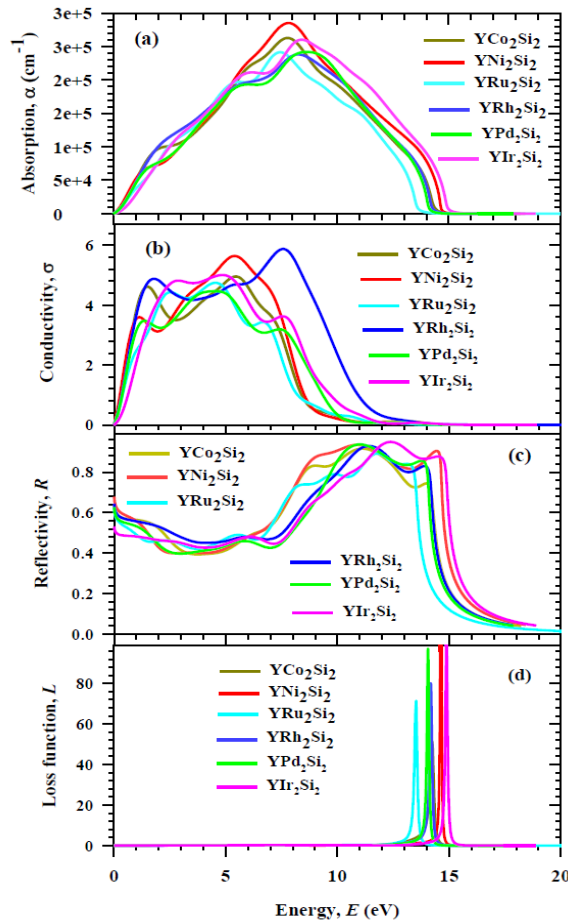


Fig. 11: (a) Absorption, (b) conductivity, (c) reflectivity and (d) loss function of YT_2Si_2 ($T=Co, Ni, Ru, Rh, Pd, Ir$).

6. Thermodynamic Properties

The several solid-state phenomena of the crystalline materials are directly described by very essential parameters called thermodynamic properties. These features included the Debye temperature, minimum thermal conductivity, melting temperature and Dulong-Petit limit. The Debye temperature is usually associated to the crystal's highest normal mode of vibration and provides deep insight into several vital thermodynamic features included thermal expansion, specific heat, melting point etc. Several approximations have been applied to determine the Debye temperature of materials. Here we have utilized the single elastic stiffness constant values to explore the Debye temperature of YT_2Si_2 (T=Co, Ni, Ru, Rh, Pd, Ir). The calculated values of Debye temperature θ_D , minimum thermal conductivity and melting temperature of YT_2Si_2 (T=Co, Ni, Ru, Rh, Pd, Ir) with some 122 type superconductors are listed in Table 7.

In a particular temperature or minimum temperature, Debye temperature is known as the maximum frequency mode of vibration. The Debye temperature (θ_D) is not an accurately calculated parameter and for this reason to evaluate the Debye temperature of a material the various data can be used but we have used to elastic modulus data to calculate the Debye temperature. By using the following equations, the Debye temperature has been estimated [86-90],

$$\theta_D = \frac{h}{k_B} \left[\left(\frac{3n}{4\pi} \right) \frac{N_A \rho}{M} \right]^{1/3} \times v_m \quad (16)$$

In this expression h and K_B indicate the Planck and Boltzman constant, N_A indicates the Avogadro's number, ρ indicates the density, M indicates as the Molecular weight and n indicates the number of atoms contained in the unit cell of (T=Co, Ni, Ru, Rh, Pd, Ir).

$$v_m = \left[\frac{1}{3} \left(\frac{2}{v_t^3} + \frac{1}{v_l^3} \right) \right]^{-1/3} \quad (17)$$

Furthermore, v_m be the average elastic (sound) wave velocity which is used in the equation of Debye temperature calculation. v_m can be determined by using the value of v_t and v_l and also known as the transverse and longitudinal sound velocities.

$$v_l = \left(\frac{3B+4G}{3\rho} \right)^{1/2} \quad (18)$$

$$v_t = \left(\frac{G}{\rho} \right)^{1/2} \quad (19)$$

The minimum thermal conductivity (K_{min}) is an essential property of solid which reveals the conduction of heat in a material. Thermal conductivity decreases for increasing the temperature and reaches at a certain point called minimum thermal conductivity [91]. The minimum thermal conductivity can be obtained by the following equation [92]:

$$K_{min} = k_B v_m \left(\frac{n N_A \rho}{M} \right)^{2/3} \quad (20)$$

Where, N is the number of atoms per unit cell and N_A is the Avogadro number. The calculated minimum thermal conductivity is listed in Table 6. For the low value of Debye temperature the minimum thermal conductivity indicates the low value according to the thumb rule [93]. The melting temperature becomes one of the important properties of a solid crystal. And the solid alters its state to liquid at atmospheric pressure and this fact is well-known as melting point of solid. At melting temperature the solid and liquid also found in equilibrium state. Fine et al. suggested the following empirical equation for cubic substance, which is applied to compute the melting temperature: [94],

$$T_m = 553 + 5.91 C_{II} \quad (21)$$

Table 5: The evaluated density ρ , transverse sound velocity v_t , longitudinal sound velocity v_l , average sound velocity v_m and Debye temperature θ_D , the minimum thermal conductivity and melting temperature of YT_2Si_2 (T=Co, Ni, Ru, Rh, Pd, Ir) with some 122 type superconductors.

Compounds	ρ (kg/m^3)	v_t (m/s)	v_l (m/s)	v_m (m/s)	θ_D (K)	K_{min} ($Wm^{-1}K^{-1}$)	T_m (K)	Ref.
YCo ₂ Si ₂	5.835	4132.81	6930.17	4574.59	553.66	1.04	1709.9	This work
YNi ₂ Si ₂	5.709	3761.59	6510.92	4179.16	501.94	0.94	1647.11	
YRu ₂ Si ₂	6.807	3526.22	6176.29	3918.56	454.44	0.87	1688.03	
YRh ₂ Si ₂	6.936	3597.99	6348.33	4000.78	465.33	0.84	1707.80	
YPd ₂ Si ₂	6.899	3001.67	5677.85	3355.38	387.01	0.69	1552.16	
YIr ₂ Si ₂	10.509	3316.67	5670.70	3677.84	428.18	0.78	2006.98	
BaNi ₂ P ₂	5.68	2513.23	4761.23	2876.93	323.70	0.56	1003.60	[33]
BaIr ₂ P ₂	9.60	2394.43	4279.87	2669.30	293.06	0.49	1257.81	[31]
BaRh ₂ Ge ₂	7.42	2217.91	3779.05	2458.68	262.07	0.43	860.85	[29]
SrRh ₂ Ge ₂	7.49	2692.52	4607.41	2985.98	330.98	0.57	1047.90	
SrRu ₂ P ₂	6.27	2918.34	4996.48	3236.66	363.86	0.63	1138.23	[30]
LaPd ₂ Ge ₂	8.09	2365.28	4559.00	2647.33	291.69	0.50	1125.93	[35]
YRh ₂ Ge ₂	8.04	2650.91	5097.71	2966.57	336.38	0.59	1306.50	[29]

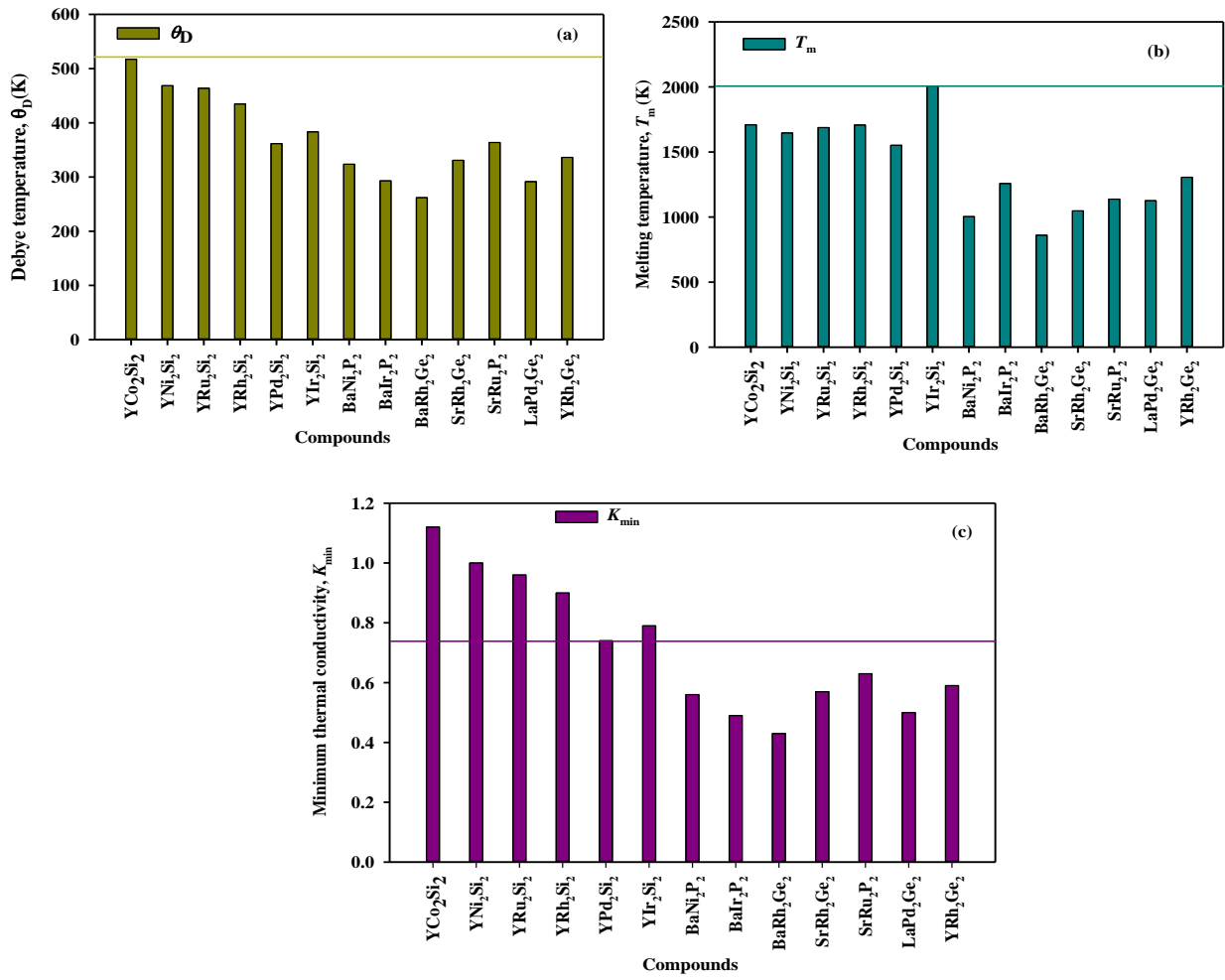


Fig.12: Thermodynamic properties of YT_2Si_2 (T=Co, Ni, Ru, Rh, Pd, Ir).

References

- [1] Braun, H. F., N. Engel, and E. Parthé. "Polymorphism and superconductivity of LaIr₂Si₂." *Physical Review B* 28, no. 3 (1983): 1389.
- [2] Kang, Dae-Bok. "A Strong Dependence of the PP Bond Length on the Transition Metal Component in ThCr₂Si₂-Type Phosphides CaM₂P₂ (M= Fe, Ni): The Influence of d Band Position and σ p* Mixing." *Bulletin of the Korean Chemical Society* 24, no. 8 (2003): 1215-1218.
- [3] Banu, IB Shameem, M. Rajagopalan, Mohammed Yousuf, and P. Shenbagaraman. "Electronic and bonding properties of ANi₂P₂ (A= Ca, Sr, Ba)." *Journal of alloys and compounds* 288, no. 1-2 (1999): 88-95.

- [4] Just, G., and P. Paufler. "On the coordination of ThCr_2Si_2 (BaAl_4 -type compounds within the field of free parameters." *Journal of alloys and compounds* 232, no. 1-2 (1996): 1-25.
- [5] Ban, Z., and M. Sikirica. "The crystal structure of ternary silicides ThM_2Si_2 ($\text{M} = \text{Cr, Mn, Fe, Co, Ni}$ and Cu)." *Acta Crystallographica* 18, no. 4 (1965): 594-599.
- [6] Shein, I. R., and A. L. Ivanovskii. "Structural, elastic, electronic and magnetic properties of ThCr_2Si_2 from first-principles calculations." *Solid state communications* 151, no. 17 (2011): 1165-1168.
- [7] Mörsen, E., B. D. Mosel, W. Müller-Warmuth, M. Reehuis, and W. Jeitschko. "Mössbauer and magnetic susceptibility investigations of strontium, lanthanum and europium transition metal phosphides with ThCr_2Si_2 type structure." *Journal of Physics and Chemistry of Solids* 49, no. 7 (1988): 785-795.
- [8] Nagarajan, R., E. V. Sampathkumaran, L. C. Gupta, R. Vijayaraghavan, V. Prabhawalkar, and B. D. Padalia. "Mössbauer and x-ray absorption spectroscopic measurements on the new mixed-valence system EuNi_2P_2 ." *Physics Letters A* 84, no. 5 (1981): 275-277.
- [9] Bauer, E. D., F. Ronning, B. L. Scott, and J. D. Thompson. "Superconductivity in SrNi_2As_2 single crystals." *Physical Review B* 78, no. 17 (2008): 172504.
- [10] Ronning, Filip, N. Kurita, E. D. Bauer, B. L. Scott, Tuson Park, Tomasz Klimczuk, R. Movshovich, and Joe D. Thompson. "The first order phase transition and superconductivity in BaNi_2As_2 single crystals." *Journal of Physics: Condensed Matter* 20, no. 34 (2008): 342203.
- [11] Reffas, Mounir, Abdelmadjid Bouhemadou, Khelifa Haddadi, Saad Bin-Omran, and Layachi Louail. "Ab initio prediction of the structural, electronic, elastic and thermodynamic properties of the tetragonal ternary intermetallics XCu_2Si_2 ($\text{X} = \text{Ca, Sr}$)." *The European Physical Journal B* 87, no. 12 (2014): 1-16.
- [12] Rotter, Marianne, Marcus Tegel, and Dirk Johrendt. "Superconductivity at 38 K in the iron arsenide ($\text{Ba}_{1-x}\text{K}_x$) Fe_2As_2 ." *Physical review letters* 101, no. 10 (2008): 107006.
- [13] Sasmal, Kalyan, Bing Lv, Bernd Lorenz, Arnold M. Guloy, Feng Chen, Yu-Yi Xue, and Ching-Wu Chu. "Superconducting Fe-based compounds ($\text{A}_{1-x}\text{Sr}_x$) Fe_2As_2 with $\text{A} = \text{K}$ and Cs with transition temperatures up to 37 K." *Physical Review Letters* 101, no. 10 (2008): 107007.
- [14] Lv, Bing, Liangzi Deng, Melissa Gooch, Fengyan Wei, Yanyi Sun, James K. Meen, Yu-Yi Xue, Bernd Lorenz, and Ching-Wu Chu. "Unusual superconducting state at 49 K in electron-doped CaFe_2As_2 at ambient pressure." *Proceedings of the National Academy of Sciences* 108, no. 38 (2011): 15705-15709.
- [15] Anand, V. K., Hyunsoo Kim, Makariy A. Tanatar, Ruslan Prozorov, and David C. Johnston. "Superconductivity and physical properties of CaPd_2Ge_2 single crystals." *Journal of Physics: Condensed Matter* 26, no. 40 (2014): 405702.
- [16] Anand, V. K., H. Kim, M. A. Tanatar, R. Prozorov, and D. C. Johnston. "Superconducting and normal-state properties of APd_2As_2 ($\text{A} = \text{Ca, Sr, Ba}$) single crystals." *Physical Review B* 87, no. 22 (2013): 224510.

- [17] Fujii, H., and A. Sato. "Superconductivity in SrPd_2Ge_2 ." *Physical Review B* 79, no. 22 (2009): 224522.
- [18] Fujii, H., and A. Sato. "Crystal structure of ternary germanides SrM_2Ge_2 (M= Ni and Ir)." *Journal of Alloys and Compounds* 487, no. 1-2 (2009): 198-201.
- [19] Vališka, Michal, Jiří Pospíšil, Jan Prokleška, Martin Diviš, Alexandra Rudajevová, and Vladimír Sechovský. "Superconductivity in the YIr_2Si_2 and LaIr_2Si_2 Polymorphs." *Journal of the Physical Society of Japan* 81, no. 10 (2012): 104715.
- [20] Karaca, Ertuğrul, Hüseyin Murat Tütüncü, G. P. Srivastava, and S. Uğur. "Electron-phonon superconductivity in the ternary phosphides BaM_2P_2 (M= Ni, Rh, and Ir)." *Physical Review B* 94, no. 5 (2016): 054507.
- [21] Shelton, R. N., H. F. Braun, and E. Musick. "Superconductivity and relative phase stability in 1: 2: 2 ternary transition metal silicides and germanides." *Solid state communications* 52, no. 9 (1984): 797-799.
- [22] Palstra, T. T. M., G. Lu, A. A. Menovsky, G. J. Nieuwenhuys, P. H. Kes, and J. A. Mydosh. "Superconductivity in the ternary rare-earth (Y, La, and Lu) compounds RPd_2Si_2 and RRh_2Si_2 ." *Physical Review B* 34, no. 7 (1986): 4566.
- [23] Nagarajan, R., Chandan Mazumdar, Zakir Hossain, S. K. Dhar, K. V. Gopalakrishnan, L. C. Gupta, C. Godart, B. D. Padalia, and R. Vijayaraghavan. "Bulk superconductivity at an elevated temperature ($T_c \approx 12$ K) in a nickel containing alloy system Y-Ni-BC." *Physical review letters* 72, no. 2 (1994): 274.
- [24] Cava, R. J., H. Takagi, H. W. Zandbergen, J. J. Krajewski, W. F. Peck, T. Siegrist, B. Batlogg et al. "Superconductivity in the quaternary intermetallic compounds $\text{LnNi}_2\text{B}_2\text{C}$." *nature* 367, no. 6460 (1994): 252-253.
- [25] Cava, R. J., B. Batlogg, T. Siegrist, J. J. Krajewski, W. F. Peck Jr, S. Carter, R. J. Felder, H. Takagi, and R. B. Van Dover. "Superconductivity in $\text{RPt}_2\text{B}_2\text{C}$." *Physical Review B* 49, no. 17 (1994): 12384.
- [26] Eyring, L., Karl A. Gschneidner, and G. H. Lander, eds. *Handbook on the physics and chemistry of rare earths*. Vol. 32. Elsevier, 2002.
- [27] Höting, Christoph, Hellmut Eckert, Samir F. Matar, Ute Ch Rodewald, and Rainer Pöttgen. "The Silicides YT_2Si_2 (T= Co, Ni, Cu, Ru, Rh, Pd): A Systematic Study by ^{89}Y Solid-state NMR Spectroscopy." *Zeitschrift für Naturforschung B* 69, no. 3 (2014): 305-312.
- [28] Shein, Igor R. "Stability, structural, elastic, and electronic properties of polymorphs of the superconducting disilicide YIr_2Si_2 ." *Physica B: Condensed Matter* 406, no. 19 (2011): 3525-3530.
- [29] Salma, M. U., and Md Atikur Rahman. "Physical properties of ThCr_2Si_2 -type Rh-based compounds ARh_2Ge_2 (A= Ca, Sr, Y and Ba): DFT based first-principles investigation." *International Journal of Modern Physics B* 32, no. 32 (2018): 1850357.
- [30] Chowdhury, Uttam Kumar, Atikur Rahman, Afjalur Rahman, Pretam Kumar Das, M. U. Salma, Shahjahan Ali, and Dayal Chandra Roy. "The physical properties of ThCr_2Si_2 -type Ru-based compounds SrRu_2X_2 (X= P, Ge, As): An ab-initio investigation." *Physica C: Superconductivity and its applications* 562 (2019): 48-55.

- [31] Rahaman, Md Zahidur, and Md Atikur Rahman. "Novel 122-type Ir-based superconductors BaIr_2M_2 (M= P and As): A density functional study." *Journal of Alloys and Compounds* 711 (2017): 327-334.
- [32] Rahaman, Md Zahidur, and Md Atikur Rahman. "ThCr₂Si₂-type Ru-based superconductors LaRu₂M₂ (M= P and As): An ab-initio investigation." *Journal of Alloys and Compounds* 695 (2017): 2827-2834.
- [33] Rahman, Md Atikur, M. Zahidur Rahaman, Md Lokman Ali, and Md Shahjahan Ali. "The physical properties of ThCr₂Si₂-type nickel-based superconductors BaNi₂T₂ (T= P, As): an ab-initio study." *Chinese Journal of Physics* 59 (2019): 58-69.
- [34] Naefa, Mst Jannatul, and Md Atikur Rahman. "Physical properties of ThCr₂Si₂-type Ni-based compounds SrNi₂M₂ (M= As and Ge): DFT based Ab-initio calculations." *Physica C: Superconductivity and its Applications* 560 (2019): 19-25.
- [35] Ali, Md Shahjahan, Md Atikur Rahman, and Md Zahidur Rahaman. "A theoretical investigation of ThCr₂Si₂-type Pd-based superconductors XPd₂Ge₂ (X= Ca, Sr, La, Nd)." *Physica C: Superconductivity and its Applications* 561 (2019): 35-44.
- [36] Payne, M.C., Teter, M.P., Allan, D.C., Arias, T.A. and Joannopoulos, A.J., 1992. Iterative minimization techniques for ab initio total-energy calculations: molecular dynamics and conjugate gradients. *Reviews of modern physics*, 64(4), p.1045.
- [37] Segall, M.D., Lindan, P.J., Probert, M.A., Pickard, C.J., Hasnip, P.J., Clark, S.J. and Payne, M.C., 2002. First-principles simulation: ideas, illustrations and the CASTEP code. *Journal of physics: condensed matter*, 14(11), p.2717.
- [38] Perdew, J.P., Burke, K. and Ernzerhof, M., 1996. Generalized gradient approximation made simple. *Physical review letters*, 77(18), p.3865.
- [39] White, J.A. and Bird, D.M., 1994. Implementation of gradient-corrected exchange-correlation potentials in Car-Parrinello total-energy calculations. *Physical Review B*, 50(7), p.4954.
- [40] Monkhorst, H.J. and Pack, J.D., 1976. Special points for Brillouin-zone integrations. *Physical review B*, 13(12), p.5188.
- [41] Pfrommer, B.G., Côté, M., Louie, S.G. and Cohen, M.L., 1997. Relaxation of crystals with the quasi-Newton method. *Journal of Computational Physics*, 131(1), pp.233-240.
- [42] Murnaghan, F.D., 1937. Finite deformations of an elastic solid. *American Journal of Mathematics*, 59(2), pp.235-260.
- [43] Gaillac, R., Pullumbi, P. and Coudert, F.X., 2016. ELATE: an open-source online application for analysis and visualization of elastic tensors. *Journal of Physics: Condensed Matter*, 28(27), p.275201.
- [44] Bouhemadou, A., R. Khenata, M. Chegaar, and S. Maabed. "First-principles calculations of structural, elastic, electronic and optical properties of the antiperovskite AsNMg₃." *Physics Letters A* 371, no. 4 (2007): 337-343.
- [45] Md. Z. Rahaman and Md. A. Rahman, "ThCr₂Si₂-type Ru-based superconductors LaRu₂M₂ (M = P and As): An ab-initio investigation," *Journal of Alloys and Compounds*, vol. 695, pp. 2827–2834, Feb. 2017, doi: 10.1016/j.jallcom.2016.11.418.

- [46] Nye, J.F., 1985. *Physical properties of crystals: their representation by tensors and matrices*. Oxford university press.
- [47] Hill, Richard, The elastic behaviour of a crystalline aggregate, *Proceedings of the Physical Society, Section A* 65.5 (1952), 349.
- [48] Ranganathan, Shivakumar I., and Martin Ostoja-Starzewski, Universal elastic anisotropy index, *Physical Review Letters* 101.5 (2008), 055504.
- [49] Chen, Xing-Qiu, et al., Modeling hardness of polycrystalline materials and bulk metallic glasses, *Intermetallics* 19.9 (2011), 1275-1281.
- [50] Wang, Xiaofei, Huimin Xiang, Xin Sun, Jiachen Liu, Feng Hou, and Yanchun Zhou. "Mechanical properties and damage tolerance of bulk $\text{Yb}_3\text{Al}_5\text{O}_{12}$ ceramic." *Journal of Materials Science & Technology* 31, no. 4 (2015): 369-374
- [8] Pugh, S. F. "XCII. Relations between the elastic moduli and the plastic properties of polycrystalline pure metals." *The London, Edinburgh, and Dublin Philosophical Magazine and Journal of Science* 45, no. 367 (1954): 823-843
- [9] Frantsevich, Ivan Nikitich. "Elastic constants and elastic moduli of metals and insulators." *Reference book* (1982)
- [10] M. I. Naher, S. H. Naqib, An ab-initio study on structural, elastic, electronic, bonding, thermal, and optical properties of topological Weyl semimetal TaX ($X = \text{P, As}$). *Scientific Reports* 11 (2021) 5592.
- [11] Z. Sun, D. Music, R. Ahuja, J.M. Schneider, Theoretical investigation of the bonding and elastic properties of nanolayered ternary nitrides. *Phys. Rev. B* 71 (2005) 193402.
- [12] L. Vitos, P.A. Korzhavyi, B. Johansson, Stainless steel optimization from quantum mechanical calculations. *Nature Mater.* 2 (2003) 25.
- [13] M. J. Phasha, P. E. Ngoepe, H. R. Chauke, D. G. Pettifor, D. Nguyen-Mann, Link between structural and mechanical stability of fcc-and bcc-based ordered Mg–Li alloys. *Intermetallics* 18 (2010) 2083.
- [14] Barsoum, Michel W., and Miladin Radovic. "Elastic and mechanical properties of the MAX phases." *Annual review of materials research* 41 (2011): 195-227

Reference

- [79] Ur Rehman, Sajid, Faheem K. Butt, Zeeshan Tariq, Fateh Hayat, Rabilah Gilani, and F. Aleem. "Pressure induced structural and optical properties of cubic phase SnSe : An investigation for the infrared/mid-infrared optoelectronic devices." *Journal of Alloys and Compounds* 695 (2017): 194-201.

- [80] F. Wooten, Optical Properties of Solids (Academic Press, New York, 1972).
- [81] Segall, M. D., Philip JD Lindan, MJ al Probert, Christopher James Pickard, Philip James Hasnip, S. J. Clark, and M. C. Payne. "First-principles simulation: ideas, illustrations and the CASTEP code." *Journal of physics: condensed matter* 14, no. 11 (2002): 2717.
- [82] <http://www.lehigh.edu/~amb4/wbi/kwardlow/conductivity.htm>.
- [83] M.Roknuzzaman,M.A.Hadi,M.J.Abden,M.T.Nasir,A.K.M.A.Islam,M.S.Ali,
- [84] M.Xu,S.Y.Wang,G.Yin,J.Li,Y.X.Zheng,L.Y.Chen,Y.Jia,Appl.Phys.Lett.89 (2006)151908.
- [85] D.W.Lynch,C.G.Olson,D.J.Peterman,J.H.Weaver,Phys.Rev.B22(1980)3991.
- [86] R.Saniz,L.H.Ye,T.Shishidou,A.Freeman,J.Phys.Rev.B74(2006)014209.
- [87] J.S.deAlmeida,R.Ahuja,Phys.Rev.B73(2006)165102.
- [88] Russell, Philip. "Photonic crystal fibers." *science* 299, no. 5605 (2003): 358-362.

